Attachment 2
Ka Band Conference
Taormina, Sicily, Oct 1999

WORLD WIDE MILLIMETER WAVE ATTENUATION FUNCTIONS FROM BARBALISCIA'S 49/22 GHz OBSERVATIONS

Paul Christopher
PFC Associates
312 Loudoun St., SW
Leesburg, VA 20175
(703) 777-3239
pfchristop@aol.com

1. BACKGROUND

Satellite communication analysts have concentrated on rain attenuation as an essential guide for frequency selection since the mid '60s. This has resulted in an emphasis on frequencies less than 6 GHz for many systems until 1984. The advantages of higher frequencies, such as higher gain at constant aperture, were unfortunately de-emphasized or even outright ignored. Fortunately, Barbaliscia, Boumis, and Martellucci of the Ugo Bordone Foundation recognized recently (1,2) that non rainy conditions may be used for many VSATs and personal systems which require only 95 to 99% availability. Their results are also applicable to many other systems, even those with high required availability, if ground site diversity or angle diversity is available.

The group at the Ugo Bordone Foundation has published many maps of zenith attenuation for non rainy conditions. The maps of Europe(1) had fascinating detail. When plotted as three dimensional attenuation maps vs Longitude and Latitude, they appeared to be saddle shaped with the rider facing East toward Russia. However, we analyze only the larger feature world wide maps for 99% non rainy conditions here. This paper first uses the 49 and 22 GHz zenith attenuation maps (2) to attempt to separate the water vapor and cloud effects. After vapor and cloud effects are estimated and separated at all longitudes and latitudes, the vapor may be substituted into integrated gaseous attenuation equations (3, 4,5) to estimate attenuation over a wide range of frequencies. World wide zenith attenuation is then estimated quantitatively for frequencies ranging from a few GHz to 90 GHz(Appendix). The immediately obvious possibility for a solution for water vapor and clouds would simply assume that the 22.2 GHz maps consisted largely of water vapor and some cloud attenuation. The 49.5 GHz maps would be assumed to consist largely of oxygen and a large cloud term, if cloud attenuation is proportional to f^2. The short equations to be solved could be concisely represented as

$$A22_{vapor} + A22_{cloud} = A22_{BarbalisciaMap} \quad \text{dB,} \quad \text{at 22.2 GHz}$$

$$\text{and} \quad A49_{O2} + A22_{cloud}\,(49/22)^2 = A49_{BarbalisciaMap} \quad \text{at 49.5 GHz} \qquad (1)$$

where two separate Barbaliscia maps (22.2 and 49.5 GHz) are used for the right sides.

If oxygen attenuation($A49_{O2}$) is chosen as a nearly constant 1.2 dB over large portions of the earth's temperate regions, the equation may be solved immediately to separate vapor and cloud attenuation at 22.2 GHz. This results in a long but useful equation (Appendix) for zenith attenuation at the 99% non rainy condition as a function of Longitude and Latitude.

A harsh note of reality intrudes when we realize that Liebe's 183 GHz water vapor line extends its effects down to the 40 GHz region. Indeed, Liebe's results imply vapor attenuation at 49 GHz as nearly 76% of the peak 22.2 GHz attenuation. The result is complicated further by an approximate water vapor attenuation equation which follows a power law relation for frequencies between 50 and 100 GHz. The exponent of the power law is close to 1.86. This added term for the second line of equation (1) presents some problems but the simultaneous solution can still proceed. A practical problem is presented instead; The resultant zenith attenuation becomes so long that it is often impractical to work with or even too long to discuss. The simple and extended solutions are shown and compared below.

2. Results for a Simple Derivation

The group at Foundation Ugo Bordone developed comprehensive attenuation maps for the whole earth at 22 and 49 GHz. Fig. 2-1 shows an approximate and smoothed form of their attenuation maps at 22.2 GHz. Fig. 2-2 shows the higher attenuation at 49.5 GHz.

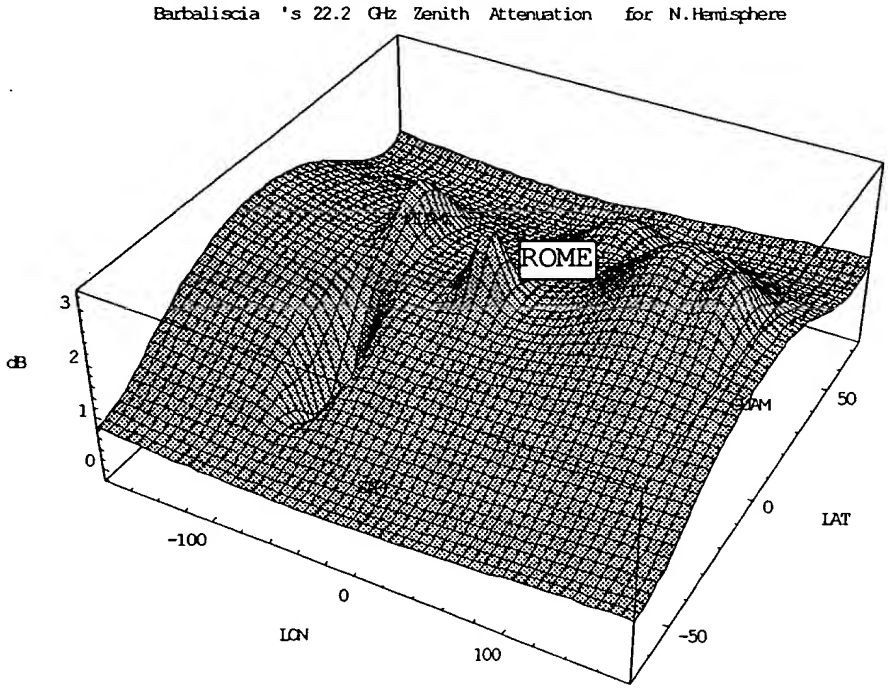

Fig. 2-1 Barbaliscia's 99% Non Rainy Zenith Attenuation at 22.2 GHz vs LON, LAT (note ROME, Miami, Guam, and S.America (SAM))

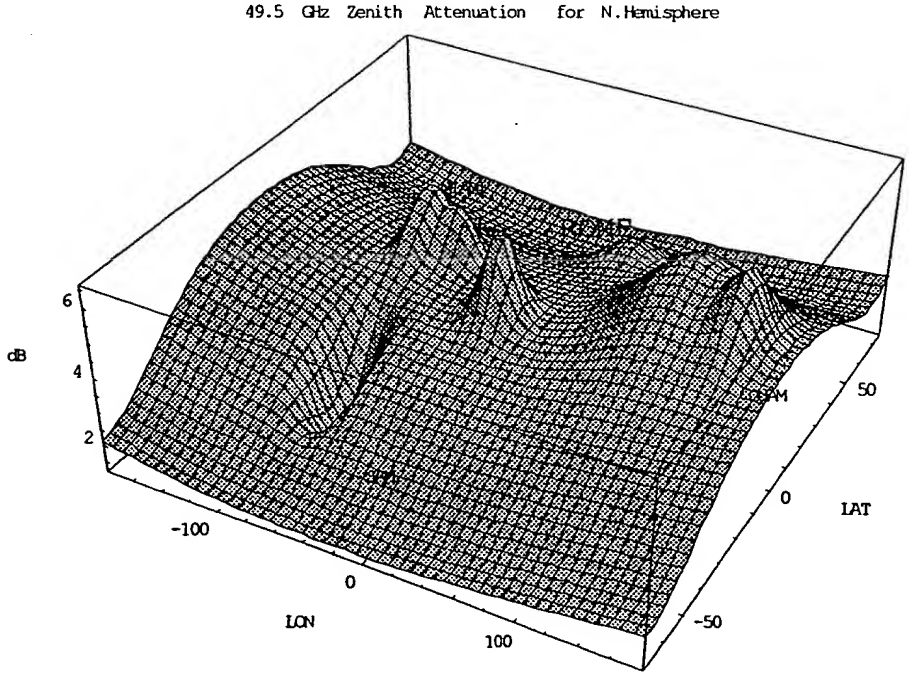

Fig. 2-2 Barbaliscia's 99% Non Rainy Zenith Attenuation at 49.5 GHz vs LON, LAT

Simple assumptions outlined above may be applied to the attenuation of Figs. 2-1 and 2-2 to derive the equation of the Appendix. Specific frequencies, such as 30 GHz, can be substituted into the equation to give Fig.2-3 and comparisons made with Barbaliscia's 30 GHz attenuation maps.

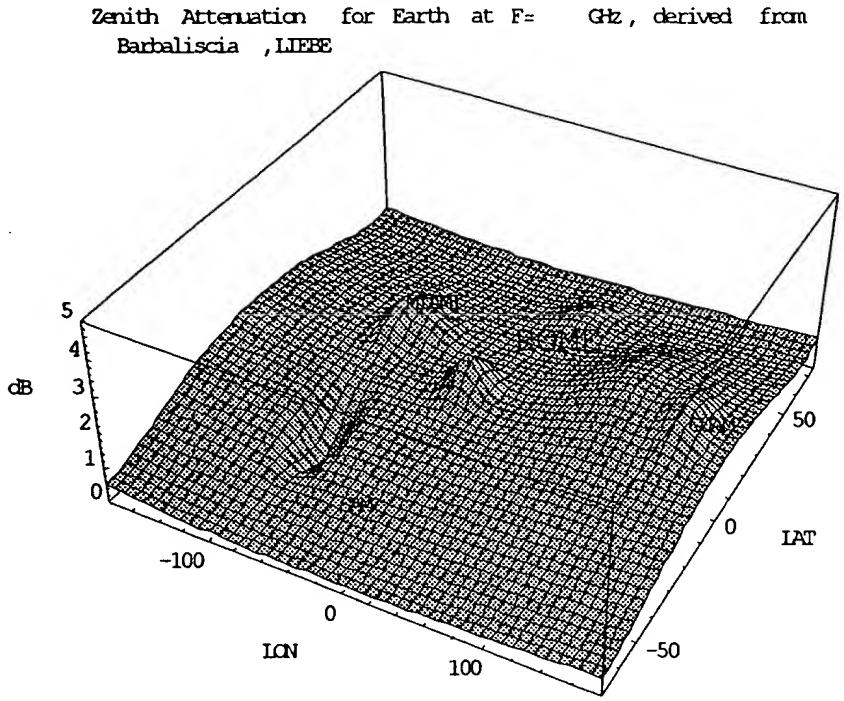

Fig. 2-3 Zenith Attenuation for 99% Non Rainy Conditions at 30 GHz From Simple Derivation (Appendix)

The world wide attenuation of Fig. 3 tends to obscure some important landmarks of the Northern Hemisphere. Fig. 2-4 includes areas only to 10 deg. South to emphasize important features as Miami, Rome, and Guam.

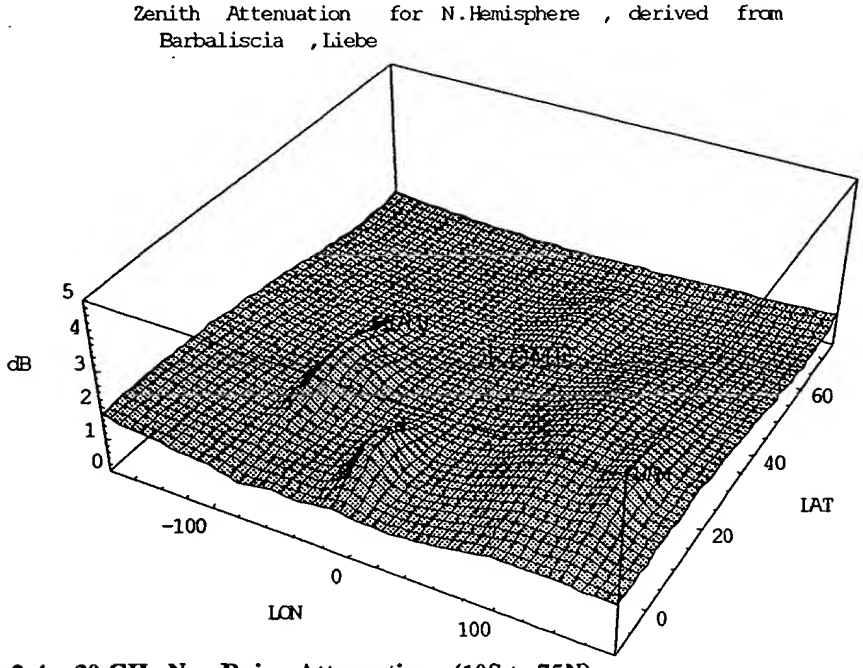

Fig. 2-4 30 GHz Non Rainy Attenuation, (10S to 75N)

It is also interesting to check the simple derivation of the Appendix at 45 GHz and 90 GHz, as Figs. 2-5 and 2-6.

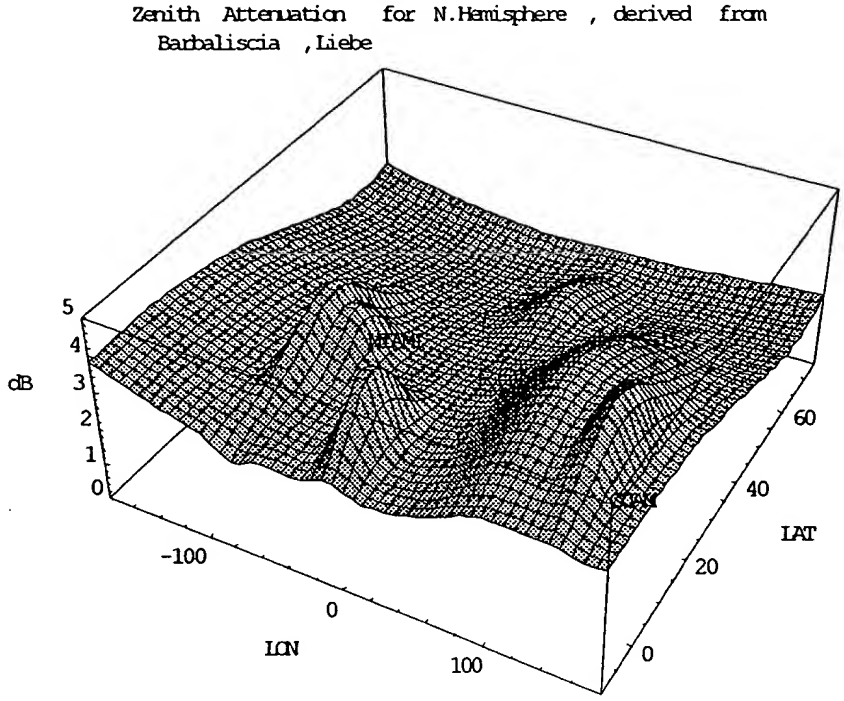

Fig. 2-5 45 GHz Zenith Attenuation for 99% Non Rainy Conditions, with Simple Assumptions (note Rome at center)

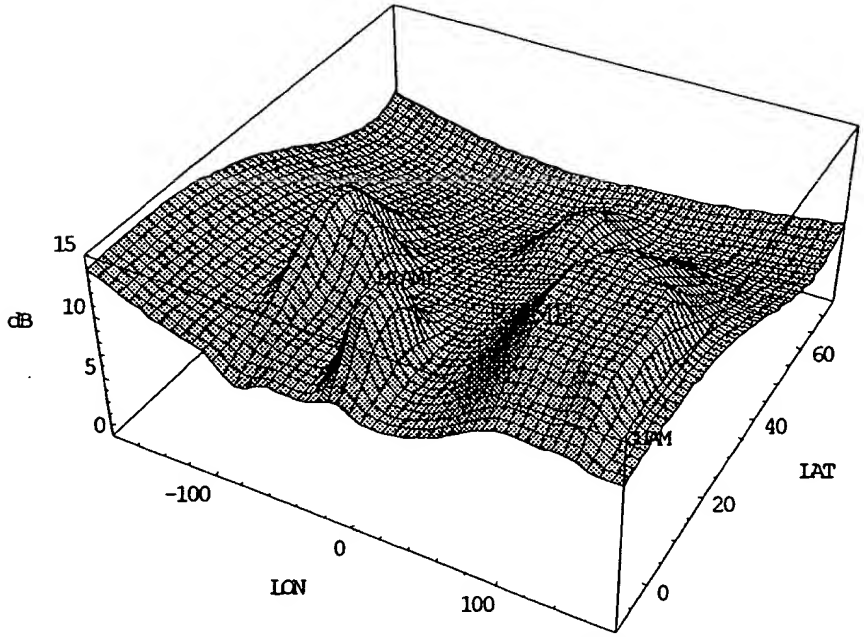

Fig. 2-6 90 GHz Zenith Attenuation Estimate, with Simple Assumptions

Comparison of Simple Assumptions with Liebe Vapor Assumptions

Liebe's 183 GHz water vapor attenuation results imply very broad vapor effects, extending to below 50 GHz. Water vapor attenuation at 50 GHz is implied to be nearly 76% of the attenuation at 22.2 GHz. An extended solution of equation (1) results in an equation much longer than that shown for the simple assumptions(Appendix). It is worthwhile to see the numerical differences introduced by the two solutions. We omit comparisons at 30 and 45 GHz, because there is very little difference between the two solutions. The 90 GHz solution introduces much more concern because it represents an extrapolation outside the data range. Fig. 2-7 shows the results for the extended Liebe solution at 90 GHz.

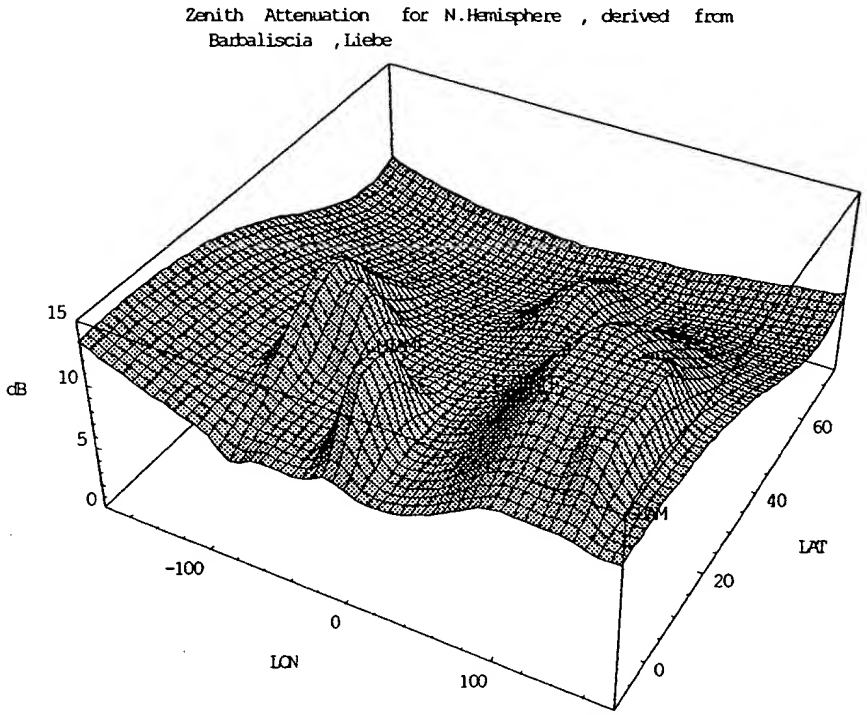

Fig. 2-7 Extended Liebe Solution for Zenith Attenuation at 90 GHz
(Compare with Fig. 2-6)

A close comparison of Fig. 2-7 with the simple solution of Fig. 2-6 shows slightly lower attenuation for Fig. 2-7. How did this close comparison happen? Part of the 49 GHz attenuation was assumed to be due to vapor while developing Fig.2-7. The Liebe vapor attenuation has a frequency exponent close to 1.86 for the 50- 100 GHz range, and this may be compared with the frequency^2 relation assumed for the clouds of the simple solution. This results in the slightly lower attenuation of Fig.2-7.

3. APPLICATIONS

The first application of the general zenith attenuation maps would be for satellites at high elevation angle. As the group at the Ugo Bardone Foundation has pointed out, attenuation maps for real satellite systems would be weighted by the cosecant(elevation). The elevation profile could be deterministic, as for a geostationary satellite, and the attenuation maps would be shaped like a deep dish with the subsatellite point(highest elevation angle) at the bottom of the dish and the attenuation curving up sharply at the edge of satellite coverage.

Or, the zenith attenuation maps could be applied to non- geostationary satellites. A Molniya system (Fig. 3-1) provides a convenient example. The inclined, elliptic orbit is shown at 1 hour increments for the 12 hour orbit. The figure suggests, and indeed it can be verified, that high elevation is seen for many hours of the orbit in the temperate regions. Three phased Molniya plus two antipodal geostationary satellites can be placed advantageously to provide high elevation throughout the Northern Hemisphere. The system is dynamic, and elevation can be represented as a probability density function vs. Latitude as Fig. 3-2.

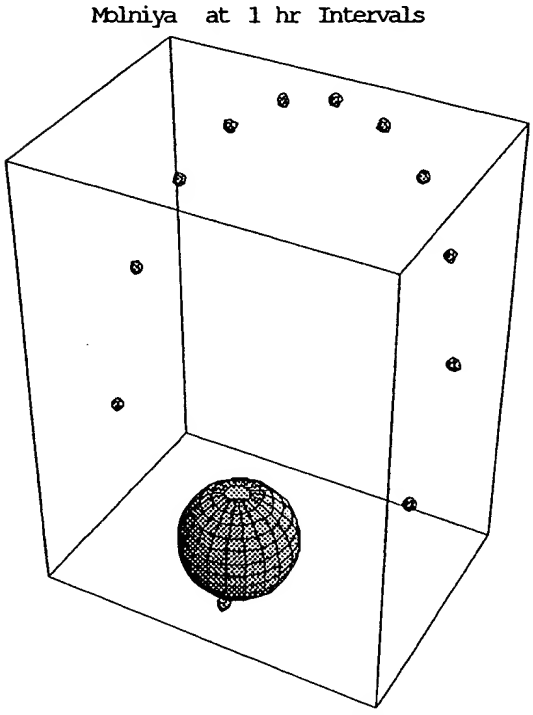

Fig. 3-1 Molniya at 1 Hr Increments

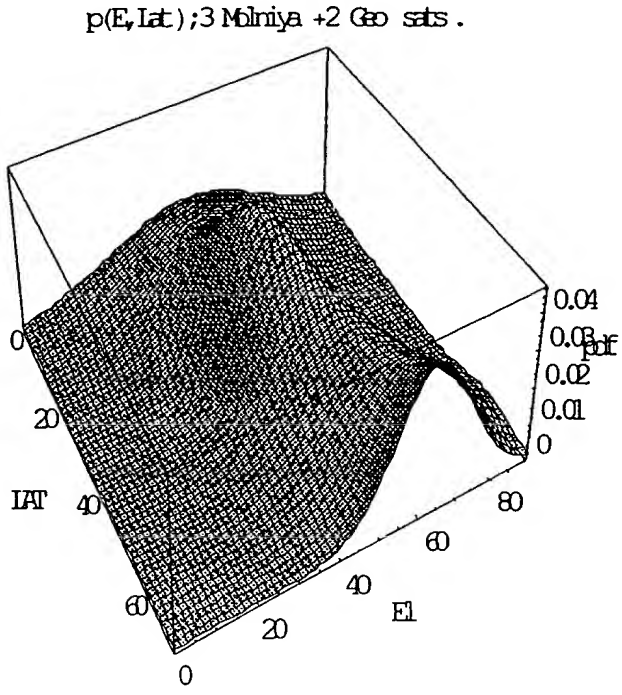

Fig. 3-2 p(Elevation) vs. Latitude for 3 Molniya + 2 Geo

Average elevation angle of Fig. 3-2 is seen to approach 60 deg. at 70 deg. North. Elevation is also tightly grouped, and elevation less than 40 degrees is unlikely at high latitudes. Average elevation approaches 50 degrees even at New York City (40N). Elevation deteriorates at low latitudes.
The elevation density function may be found with Mathematica as:

$$p(\text{Elevation}) = \frac{E^{-\frac{(-47.0509+0.165865\,LAT+0.00512491\,LAT^2-0.000520006\,LAT^3+5.22822\times10^{-6}\,LAT^4+x)^2}{2\left(-160.041+181.722\,E^{-\frac{LAT^2}{900}}-0.776901\,LAT+0.270942\,LAT^2-0.00526509\,LAT^3+0.000029238\,LAT^4\right)^2}}}{\left(-160.041+181.722\,E^{-\frac{LAT^2}{900}}-0.776901\,LAT+0.270942\,LAT^2-0.00526509\,LAT^3+0.000029238\,LAT^4\right)\sqrt{2\pi}}$$

The right side has elevation represented by x for conciseness.
The density function is weighted by attenuation before applying it to the zenith attenuation maps. After weighting by cosecant(elevation), the average attenuation at each latitude corresponds to a lower elevation than average elevation. For example, a 60 deg. average elevation with 14 deg. standard deviation might deliver an average attenuation corresponding to less than 55 degrees as a result of the nonlinear transformation.

The elevation density function may be applied to the zenith attenuation maps, to give comparisons similar to Figs. 3-3 and 3-4. Fig. 3-4 is seen to give much higher attenuation at low latitudes due to low Molniya elevation near the equator.

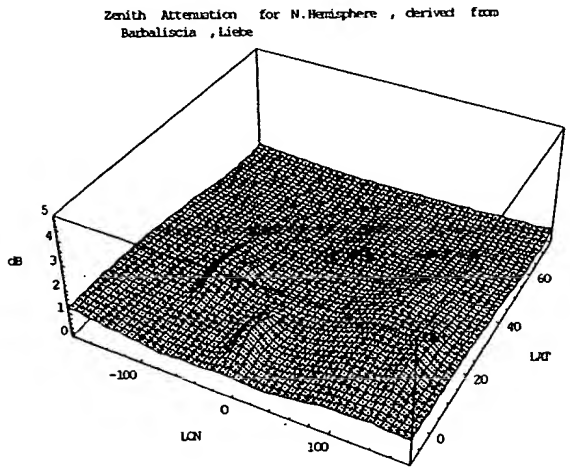

Fig. 3-3 Zenith Attenuation at 30 GHz

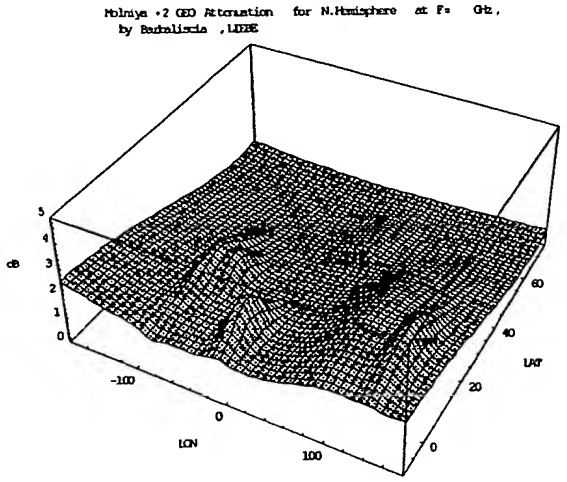

Fig. 3-4 Molniya Attenuation at 30 GHz

Attenuation as a function of frequency may also be plotted at interesting locations. Further, the net loss (attenuation minus antenna gain at constant aperture) may be plotted to estimate attractive frequency regions. Figure 3-5 shows net loss for Rome, where 42 GHz appears attractive with low net loss.

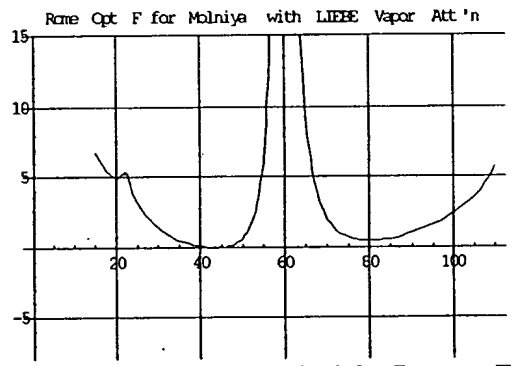

Fig. 3-5 Molniya Net Loss(dB) for Rome vs F

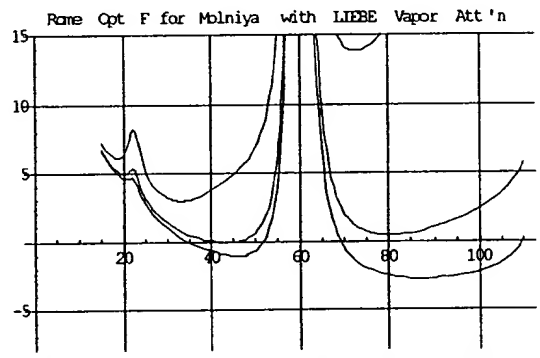

Fig. 3-6 Molniya Net Loss for Guam,Rome,Oslo

More difficult and more benign areas may also be compared. Fig. 3-6 shows Guam as the top curve, and the global minimum net loss appears near 36 GHz. Rome is seen as the middle curve. Oslo presents another interesting region, where 90 GHz appears most attractive.

4. CONCLUDING THOUGHTS

We have shown that Barbaliscia's zenith attenuation maps offer at least two interesting possibilities for separating cloud and water vapor effects. A simple solution (Appendix) gave a long but useful equation for zenith attenuation at a wide range of frequencies from 70 deg. South to 75 deg. North. A more comprehensive Liebe solution resulted in a much longer general answer and slightly lower attenuation at 90 GHz. An application of the zenith attenuation maps to an NGO system was shown, along with a method for finding attractive frequencies. The Barbaliscia results often imply that frequencies greater than 40 GHz are attractive.

5. REFERENCES

1. F. Barbaliscia, M. Boumis, A. Martellucci, "Characterization of Atmospheric Attenuation in the Absence of Rain in Europe in SHF/EHF Bands for VSAT Satcom Systems Applications," Ka Band Conference, Sorrento, Italy, Sept. 1997.

2. F. Barbaliscia, M. Boumis, A. Martellucci, "World Wide Maps of Non Rainy Attenuation for Low-Margin Satcom Systems Operating in SHF/EHF Bands," Ka Band Conference, Sept. 1998.
3. A.K. Kamal, P. Christopher, "Communication at Millimeter Wavelengths," Proc. ICC, Denver, 1981.
4. H. J. Liebe, P.W. Rosencranz, G.A. Hufford, "Atmospheric 60 GHz Oxygen Spectrum: New Laboratory Measurements—," J. Quantum Spectroscopy and Radiative Transfer, Vol.48, 1992
5. A.H. Jackson, P. Christopher, "A LEO Concept for Millimeter Wave Communication," Proc. IMSC, Ottawa, June 1995.
6. S. Wolfram, Mathematica A System for Doing Mathematics by Computer, 3rd Edition, 1997.

Appendix Global Equation for Non Rainy Zenith Attenuation, without Liebe's Vapor Attenuation in 40- 100 GHz Region

LIEBE azen=

$$0.000408122\,fg^2\left(5.34566+1.48098\,E^{-\frac{1}{200}(-10+LAT)^2-\frac{1}{200}(-145+LON)^2}+2.03295\,E^{-\frac{1}{800}(-18+LAT)^2-\frac{(-102+LON)^2}{1800}}+\right.$$
$$1.1968\,E^{-\frac{1}{200}(-52+LAT)^2-\frac{1}{800}(-28+LON)^2}-2.78685\,E^{-\frac{LAT^2}{1800}-\frac{LON^2}{180000}}+2.48024\,E^{-\frac{1}{72}(-2+LAT)^2-\frac{1}{200}(7+LON)^2}+$$
$$1.41803\,E^{-\frac{1}{50}(-20+LAT)^2-\frac{1}{200}(60+LON)^2}-2.26449\,E^{-\frac{1}{200}(28+LAT)^2-\frac{1}{200}(77+LON)^2}+$$
$$1.69839\,E^{-\frac{1}{200}(-20+LAT)^2-\frac{1}{128}(82+LON)^2}+0.000898808\,LAT-0.00187405\,LAT^2+8.15535\times10^{-7}\,LAT^3+$$
$$1.92203\times10^{-7}\,LAT^4-0.000690105\,LON-5.83206\times10^{-6}\,LAT\,LON+3.42574\times10^{-7}\,LAT^2\,LON+$$
$$\left.0.0000243378\,LON^2+1.15354\times10^{-8}\,LAT\,LON^2-3.5046\times10^{-8}\,LON^3-6.44437\times10^{-11}\,LON^4\right)+$$

$$0.00586939\,fg^2\left(3.14686+0.665394\,E^{-\frac{1}{200}(-10+LAT)^2-\frac{1}{200}(-145+LON)^2}+\right.$$
$$1.1188\,E^{-\frac{1}{800}(-18+LAT)^2-\frac{(-102+LON)^2}{1800}}+0.716478\,E^{-\frac{1}{200}(-52+LAT)^2-\frac{1}{800}(-28+LON)^2}-$$
$$1.18012\,E^{-\frac{LAT^2}{1800}-\frac{LON^2}{180000}}+1.21591\,E^{-\frac{1}{72}(-2+LAT)^2-\frac{1}{200}(7+LON)^2}-1.89544\,E^{-\frac{1}{200}(28+LAT)^2-\frac{1}{200}(77+LON)^2}+$$
$$0.8941\,E^{-\frac{1}{200}(-20+LAT)^2-\frac{1}{128}(82+LON)^2}+0.00101461\,LAT-0.000943554\,LAT^2+2.75301\times10^{-7}\,LAT^3+$$
$$1.00142\times10^{-7}\,LAT^4-0.000268921\,LON-1.63982\times10^{-6}\,LAT\,LON+2.33496\times10^{-7}\,LAT^2\,LON+$$
$$0.0000108872\,LON^2+1.02349\times10^{-8}\,LAT\,LON^2-1.77808\times10^{-8}\,LON^3-1.11299\times10^{-10}\,LON^4-$$
$$0.201139\left(5.34566+1.48098\,E^{-\frac{1}{200}(-10+LAT)^2-\frac{1}{200}(-145+LON)^2}+2.03295\,E^{-\frac{1}{800}(-18+LAT)^2-\frac{(-102+LON)^2}{1800}}+\right.$$
$$1.1968\,E^{-\frac{1}{200}(-52+LAT)^2-\frac{1}{800}(-28+LON)^2}-2.78685\,E^{-\frac{LAT^2}{1800}-\frac{LON^2}{180000}}+2.48024\,E^{-\frac{1}{72}(-2+LAT)^2-\frac{1}{200}(7+LON)^2}+$$
$$1.41803\,E^{-\frac{1}{50}(-20+LAT)^2-\frac{1}{200}(60+LON)^2}-2.26449\,E^{-\frac{1}{200}(28+LAT)^2-\frac{1}{200}(77+LON)^2}+$$
$$1.69839\,E^{-\frac{1}{200}(-20+LAT)^2-\frac{1}{128}(82+LON)^2}+0.000898808\,LAT-0.00187405\,LAT^2+8.15535\times10^{-7}\,LAT^3+$$
$$1.92203\times10^{-7}\,LAT^4-0.000690105\,LON-5.83206\times10^{-6}\,LAT\,LON+3.42574\times10^{-7}\,LAT^2\,LON+$$
$$\left.\left.0.0000243378\,LON^2+1.15354\times10^{-8}\,LAT\,LON^2-3.5046\times10^{-8}\,LON^3-6.44437\times10^{-11}\,LON^4\right)\right)$$

$$\left(0.665418-132.118\,(-0.740741+0.0333667\,fg)^2\right.$$
$$\left.\left(0.999375-11.4943\sqrt{(-0.740741+0.0333667\,fg)^2}\,\text{ArcTan}\left[\frac{0.0869456}{\sqrt{(-0.740741+0.0333667\,fg)^2}}\right]\right)-$$
$$132.118\,(0.740741+0.0333667\,fg)^2$$
$$\left.\left.\left(0.999375-11.4943\sqrt{(0.740741+0.0333667\,fg)^2}\,\text{ArcTan}\left[\frac{0.0869456}{\sqrt{(0.740741+0.0333667\,fg)^2}}\right]\right)\right)-$$

$$0.00392386\,fg^2\left(18.2482\left(\text{Log}\left[\frac{(2-0.0333667\,fg)^2}{0.000749822+(2-0.0333667\,fg)^2}\right]+\right.\right.$$
$$\text{Log}\left[\frac{(3.959999999999999-0.0333667\,fg)^2}{0.000187456+(3.959999999999999-0.0333667\,fg)^2}\right]+$$
$$\text{Log}\left[\frac{\left(\frac{fg}{10}-0.0333667\,fg\right)^2}{0.000187456+\left(\frac{fg}{10}-0.0333667\,fg\right)^2}\right]+\text{Log}\left[\frac{(2+0.0333667\,fg)^2}{0.000749822+(2+0.0333667\,fg)^2}\right]+$$
$$\text{Log}\left[\frac{(3.959999999999999+0.0333667\,fg)^2}{0.000187456+(3.959999999999999+0.0333667\,fg)^2}\right]+$$
$$\left.\left.\text{Log}\left[\frac{\left(\frac{fg}{10}+0.0333667\,fg\right)^2}{0.000187456+\left(\frac{fg}{10}+0.0333667\,fg\right)^2}\right]\right)+$$
$$\left.27.7778\,\text{Log}\left[\frac{0.00111334\,fg^2}{0.000323595+0.00111334\,fg^2}\right]\right)$$